Ultrafast microwave hydrothermal synthesis and characterization of Bi1-xLaxFeO3 micronized particles

Ponzoni, C.; Cannio, M.; Boccaccini, Dino; Bahl, C. R. H.; Agersted, Karsten; Leonelli, C.

Published in:
Materials Chemistry and Physics

Link to article, DOI:
10.1016/j.matchemphys.2015.05.002

Publication date:
2015

Document Version
Publisher's PDF, also known as Version of record

Materials Chemistry and Physics 162 (2015) 69–75

Contents lists available at ScienceDirect

Materials Chemistry and Physics

journal homepage: www.elsevier.com/locate/matchemphys

Ultrafast microwave hydrothermal synthesis and characterization of $Bi_{1-x}La_xFeO_3$ micronized particles

C. Ponzoni [a], M. Cannio [a, *], D.N. Boccaccini [b], C.R.H. Bahl [b], K. Agersted [b], C. Leonelli [a]

[a] Department of Engineering "Enzo Ferrari", University of Modena and Reggio Emilia, Modena 42025, Italy
[b] Department of Energy Conversion and Storage, Technical University of Denmark Frederiksborgvej, 4000 Roskilde, Denmark

HIGHLIGHTS

- MW hydrothermal method applied to synthesize $Bi_{1-x}La_xFeO_3$, x = 0, 0.15, 0.30, 0.45.
- A single-phase perovskite structure for all the samples was confirmed by XRD.
- A T_c shift in La doped $BiFeO_3$ DTA was observed as function of the La-doping.
- Magnetic measurements indicate that the materials are weakly ferromagnetic.

GRAPHICAL ABSTRACT

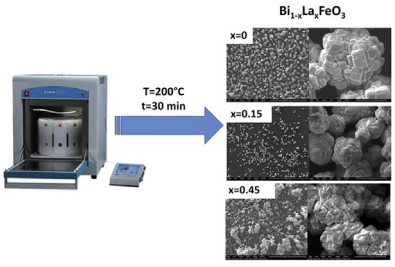

ARTICLE INFO

Article history:
Received 20 December 2014
Received in revised form
16 April 2015
Accepted 1 May 2015
Available online 5 July 2015

Keywords:
Inorganic compound
Oxides
Chemical synthesis

ABSTRACT

In this work a microwave assisted hydrothermal method is applied to successfully synthesize lanthanum doped bismuth ferrites (BLFO, $Bi_{1-x}La_xFeO_3$ where x = 0, 0.15, 0.30 and 0.45). The growth mechanism of the $Bi_{1-x}La_xFeO_3$ crystallites is discussed in detail. The existence of the single-phase perovskite structure for all the doped samples is confirmed by the X-ray powder diffraction patterns. A peak shift, observed at lower angle with increasing La doping concentration, indicates that the $BiFeO_3$ lattice is doped. The results of TG/DTA show a shift in the transition temperature from 805 °C to 815 °C as function of the La-doping for all the doped powders. At higher levels of La doping, *i.e.* x = 0.30 and 0.45, significant weight losses occur above 860 °C suggesting a change in the physical and chemical properties. Finally, magnetic measurements are carried out at room temperature for pure $BiFeO_3$ and $Bi_{0.85}La_{0.15}FeO_3$. The results indicate that the materials are both weakly ferromagnetic, with no significant hysteresis in the curves.

1. Introduction

Magnetoelectric multiferroic materials exhibit magnetic and ferroelectric order in the same temperature range [1]. In this class of compounds, ABO_3 perovskites, where A = Bi and B = first row transition metal, deserve greater attention since their multiferroic characteristics. In particular the coupling between magnetism and electric polarization of $BiFeO_3$ (BFO) has resulted in great research interest and an increasing demand for its application in several fields of science and technology such as spintronics, high-density storage media and stable nanoscale memory elements [2–5]. According to recent studies BFO, having a suitable band gap (~2.2 eV) and excellent chemical stability, is also an important UV responsive semiconductor photocatalyst used for degradation of organic pollutants [6–8]. However, potential applications of BFO are greatly limited due to the presence of impurity phases, small spontaneous polarization, high coercive field, inhomogeneous magnetic spin

* Corresponding author.
E-mail address: maria.cannio@unimore.it (M. Cannio).

http://dx.doi.org/10.1016/j.matchemphys.2015.05.002
0254-0584/

structure, ferroelectric reliability and high defect density, low insulation resistance caused by the reduction of Fe^{3+} species to Fe^{2+} and oxygen vacancies for charge compensation [9]. To tackle the leakage current issue of BFO, several research groups have attempted to partially substitute the Bi in the tetrahedral or octahedral sites of BFO by lanthanide elements (La, Ce, Nd, Sm, Eu, Gd, Tb, Dy, etc), transition metal and alkaline earth metal. This doping by non volatile ions controls the volatile nature of Bi in BFO, reduces the generation of oxygen vacancies and breaks the long-range cycloidal spin arrangement responsible for cancelling the magnetization in the rhombohedrally distorted perovskite structure [10–12].

The synthesis of complex oxide systems still remain a challenge due to the multiplicity of oxidation states, morphologies and phases. Most perovskite based materials are prepared by solid–state reactions between the corresponding oxides at temperature above 1000 °C. Other preparation procedures for perovskites and in particular for $BiFeO_3$ are sol–gel method [13], Pechini method [14], auto combustion, chemical co-precipitation method including solvothermal [15] and hydrothermal [16] synthesis. One of the major underlined problems in the preparation of single phase bismuth ferrite perovskite-type structured is the formation of impurities in both the micrometer-sized and nanostructure regions. Many studies in fact describe the formation of secondary phases such as Bi_2O_3, sillenite-type $Bi_{25}FeO_{40}$ and mullenite-type $Bi_2Fe_4O_9$ [12–15]. Moreover, the Bi perovskites under high temperatures decompose into the parent oxides [12–15]. Finally, αBi_2O_3, the intermediate compound necessary for the BFO and doped BFO formation, easily evaporates when heated at high temperature. On the other hand, at room temperature under applied fields of about 200 $kVcm^{-1}$ BFO and doped with different metals (*i.e.* La, Ag, Ca, Mn, etc) BFO can decompose, leading to hematite Fe_2O_3 [1,17,18]. J. Prado-Gonjal et al. [19] compared three different methods for preparing $BiFeO_3$ polycrystals: hydrothermal synthesis, microwave heating in the solid state and the combination of both, that is a hydrothermal method using microwave heating. The results suggest that the best materials, without high purity reactants, are obtained in few minutes by the last procedure. In our previous work [20], the facile microwave hydrothermal synthesis route for BFO, reported in [19] too, was repeated and optimized by carefully controlling the reaction conditions (alkali medium concentration, precursors ratio, temperature and time of reaction). Briefly, the results of this investigation suggest operating at 200 °C and using KOH concentration as mineralizer source ranging from 4 M to 8 M, a ratio 1/1 for the metallic nitrate precursors and a time reaction of 30 min are the best reaction conditions to prepare BFO pure-phase. All in all, these two paper indicate the microwave hydrothermal synthesis as a new, very fast, reproducible and environment-friendly method to prepare pure BFO. Based on the authors' knowledge dielectric heating with microwave assisted equipment has never been applied to the synthesis of La-doped bismuth ferrite. Here in this paper we study the microwave assisted hydrothermal synthesis: a fast co-precipitation reaction involving the simultaneous occurrence of nucleation, growth, coarsening, and eventually agglomeration processes which could represent a novel approach to prepare nanostructures lanthanum doped bismuth ferrite (BLFO). The main characteristic of this synthetic process is, in fact, its widely recognized ability to enhance powder crystallinity leading to a very homogenous particle size distribution with respect to the conventional hydrothermal approach [21,22]. Indeed when dielectric heating is applied via microwave (MW) irradiation, the homogeneity of the temperature distribution reached inside the reaction batch strongly favours the homogeneous versus heterogeneous nucleation mechanism. These advantages are even more evident if compared with the “ceramic route”, where extended periods dedicated to grinding and firing of solid precursors followed by annealing are necessary. The aim of this paper is to report the efficiency of the microwave assisted hydrothermal approach to obtain single-phase lanthanum modified bismuth ferrite powders $Bi_{1-x}La_xFeO_3$ (BLFO) with x = 0, 0.15, 0.30 and 0.45. The use of a multi-mode MW applicator equipped with temperature and pressure control system permitted a careful and detailed study of the influence of the experimental conditions (heating rate, temperature and pressure into the reactor) on the BLFO phase purity and properties. Moreover the total control of the above mentioned experimental variables allowed a very good reproducibility of the optimized process performed at 200 °C in terms of phase purity and particle size. In particular, as shown in our previous paper [20], precursors composition, mineralizer concentration, hydrothermal temperature, heating rate and time play important roles in the synthesis of these perovskites on the crystallinity and morphology of $Bi_{1-x}La_xFeO_3$ crystallites.

2. Experimental section

2.1. Materials and microwave-assisted hydrothermal method

All the analytical grade (≥99.7%) chemicals used, bismuth nitrate, $Bi(NO_3)_3 \cdot 5H_2O$, iron nitrate, $Fe(NO_3)_3 \cdot 9H_2O$, lanthanum nitrate $La(NO_3)_3 \cdot 6H_2O$ and potassium hydroxide, KOH, were purchased from Sigma Aldrich (Milan, Italy) and used without further purification of analytical grade.

$Bi_{1-x}La_xFeO_3$ micronized particles with $x = 0, 0.15, 0.30$ and 0.45 were prepared from the nitrate salts as cation precursors and KOH as miniralizer via a microwave assisted hydrothermal method optimized by our research group for undoped compounds [20].

$Bi(NO_3)_3 \cdot 5H_2O$, $La(NO_3)_3 \cdot 6H_2O$, $Fe(NO_3)_3 \cdot 9H_2O$ were added to a 8 M KOH aqueous solution in a Teflon® reaction vessel under vigorous magnetic stirring.

The vessel was placed in an ETHOS TC (Milestone Italia, Bergamo, Italy) multimode microwave applicator, operating at the frequency of 2.45 GHz and equipped with temperature and pressure monitoring devices. The reaction mixture was heated up to 200 °C in 15 min then this temperature was maintained for 30 min. The source power was 500 Watt (for two vessels). After cooling down to room temperature, the products were centrifuged and washed several times with 1 M HNO_3 deionized water solution to eliminate impurities and un-reacted starting compounds, and finally dried at 110 °C overnight in a conventional oven.

2.2. Powder characterization techniques

The dried powders were characterized by X-ray diffraction (XRD) analysis (PANAlytical, X'Pert PRO diffractometer, Almelo, The Netherlands) using Ni-filtered Cu Ka radiation (k = 1.5405 Å). The XRD patterns were collected, in the range 10°–90° at room temperature, to investigate the crystal structures of BFO with different La doping proportions.

The powder morphologies were examined by Scanning Electron Microscopy (Scanning Electron Microscopy (ESEM, Quanta-200 Fei, Oxford Instruments)) after Au sputtering.

Thermal analysis was performed using a differential thermal analyzer (DTA) (STA 429 CD, NETZSCH, Selb, Germany) to study the phase transition. All the samples were placed in alumina-crucibles and the measurements were performed with a heating/cooling rate of 10 °C/min from room temperature to ~900 °C in nitrogen atmosphere. The thermo-balance was flushed for 15 min with nitrogen prior to heating.

Raman spectra were acquired using a spectrometer equipped with an He–Ne laser illumination (Horiba Jobin Yvon LabRAM,

Kyoto, Japan). The different spectra are the average of five spectra collected consecutively in the same range, between 4000 and 100 cm^{-1}, with an excitation wavelength of 632 nm and a spectral resolution of 4 cm^{-1} with a power of 10 mW.

A vibrating sample magnetometer (VSM 7407, Lake Shore Cryotronics, OH, USA) was used to obtain the hysteresis loops (1.5T -> −1.5T -> 1.5T) for the magnetic studies of samples. All the measurements were done at room temperature using about 70 mg of each samples.

3. Results and discussion

3.1. Chemical and physics powder characterizations: formation mechanism

X-ray diffraction (XRD) was carried out to investigate the crystal structures of the BFO micronized powders with different La doping proportions ($Bi_{1-x}La_xFeO_3$ where $x = 0$, 0.15, 0.30 and 0.45), and also to check the presence of various impurities in the samples. As shown in Fig. 1, reporting the XRD patterns of the prepared $Bi_{1-x}La_xFeO_3$, all the peaks recorded for the sample with x = 0.00 confirmed the formation of pure $BiFeO_3$ (JCPDS card 00-020-169); this compound is characterized by a rhombohedrally distorted perovskite structure belonging to R3c space group. The powder diffraction of all the other samples showed the presence of a single-phase $Bi_{1-x}La_xFeO_3$ crystallizing in the same structure as the parent $BiFeO_3$ compound without any secondary or impurity phases: γ-Fe_2O_3, $Bi_2Fe_4O_9$, $Bi_{36}Fe_2O_{57}$, which often constitute the main impurity phase of BFO, were not detected. The absence of secondary phases explains the authenticity of the chosen method of preparation for BFO and BFLO.

At this point some consideration on the synthesis mechanism of the microwave assisted hydrothermal approach can be drawn, even

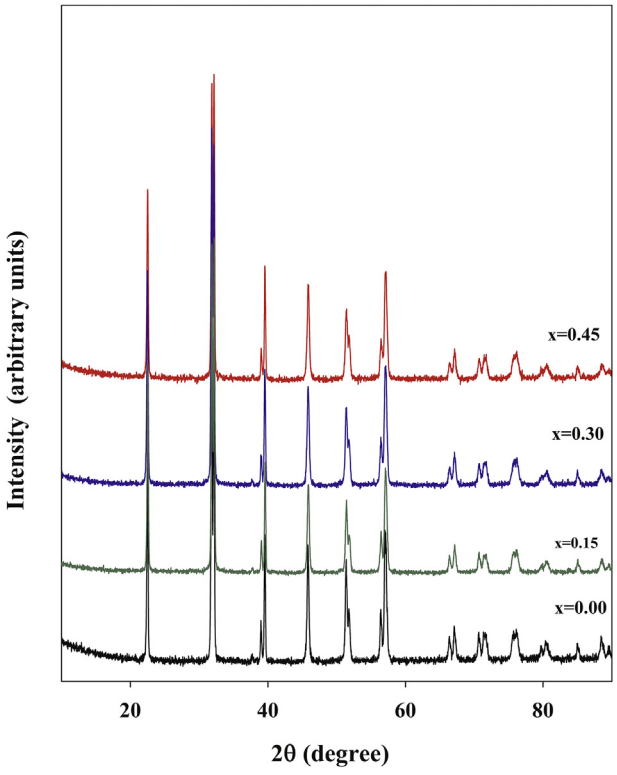

Fig. 1. XRD patterns of $Bi_{1-x}La_xFeO_3$ where x = 0, 0.15, 0.30 and 0.45 synthesized using 8 M KOH at 200 °C for 30 min.

though there is no literature evidence of its application to the synthesis of lanthanum doped bismuth ferrite. It is generally agreed that the crucial points of the based bismuth ferrite perovskites synthesis are the dissolution of the precursors (*i.e.* $Bi(NO_3)_3 \cdot 5H_2O$, $La(NO_3)_3 \cdot 6H_2O$, $Fe(NO_3)_3 \cdot 9H_2O$) and of α-bismuth oxide (reactive intermediate), vital processes to reach the *super-saturation*. The basic mechanism to describe this processes is "dissolution–crystallization" [16], in which the dissolution of the reactants is strongly dependent on a mineralizer *i.e.* KOH, and crystallization only occurs in the supersaturated fluid.

As we observed in our previous work, and in agreement with literature, the alkali concentration in synergic cooperation with high temperature and high pressure, plays a key role in the whole process as responsible of the crucial substrates dissolution [20]. In fact, with high alkali concentration (>8 M) the dissolution of the nitrate-precursors and of the reaction intermediate αBi_2O_3 are promoted. This brings to the Bi^{3+} ions formation, which reacts with $Fe(OH)_3$ leading to the $BiFeO_3$ multiferroic phase [16,19,20]. The crucial step is the achievement of the so-called *super-saturated* fluid condition in which the Bi^{3+} concentration in the alkali solution exceeds the saturation point, as detailed in Equation (2) of mechanism detailed below. Rod-like α-Bi_2O_3 particles gradually dissolve into Bi^{+3} ions, and this higher degree of *super-saturation*, useful to overpass the energetic barrier, results in a higher nucleation rate of BLFO. Finally, as indicated in Equation (3), they eventually react with amorphous iron and lanthanum (III) hydroxide leading to the $Bi_{1-x}La_xFeO_3$ multiferroic phase.

$$Bi(NO_3)_3 + La(NO_3)_3 + Fe(NO_3)_3 + 9KOH \rightarrow Bi(OH)_3 + Fe(OH)_3 + La(OH)_3 + 9KNO_3 \quad (1)$$

$$\alpha\text{-}Bi_2O_3 + 6KOH \rightarrow 2Bi(OH)_3 + 3K_2O \quad (2)$$

$$_{(1-x)}Bi(OH)_3, + {}_xLa(OH)_3 + Fe(OH)_3 \rightarrow Bi_{1-x}La_xFeO_3 + 3H_2O \quad (3)$$

$$Bi(OH)_3 + 4Fe(OH)_3 \rightarrow Bi_2Fe_4O_9 + 9H_2O \quad (4)$$

$$36Bi(OH)_3 + 2Fe(OH)_3 \rightarrow Bi_{36}Fe_2O_{57} + 57H_2O \quad (5)$$

However, it is worthwhile to remark that high concentrations of KOH (>10 M) could cause the formation of secondary phases, Equations (4) and (5), probably due to a different thermodynamic state or to kinetic reasons connected to "dissolution and crystallization process" originating from higher pH value and solubility of α-Bi_2O_3 [16,22].

Other parameters that can promote the α-Bi_2O_3 dissolution and enhance the BLFO formation are: reaction temperature, heating rate, reaction time and presence of an inorganic agent as Na_2CO_3 [19]. As said, only when the system exceeds a threshold temperature, the *super-saturation* is reached and the energy barrier transition leading to the BLFO formation. Even though the increase of the reaction time is another considered strategy to improve the dissolution of α-Bi_2O_3, the drawback is the degradation of BLFO and the formation of secondary phases ($Bi_{25}FeO_{40}$, $Bi_2Fe_4O_9$, Fe_2O_3) [16,22].

3.2. Morphology characterization

In order to investigate the morphology of the micronized particles synthesized SEM observations were performed.

Fig. 2 a–c show SEM images of $Bi_{1-x}La_xFeO_3$ ($0 \leq x \leq 0.45$) particles for selected samples. All the powders are found to be micron-sized particles that are agglomerates of micronized grains. The size and morphologies of these samples are affected by the lanthanum doping level: the images of un-doped $BiFeO_3$ particles

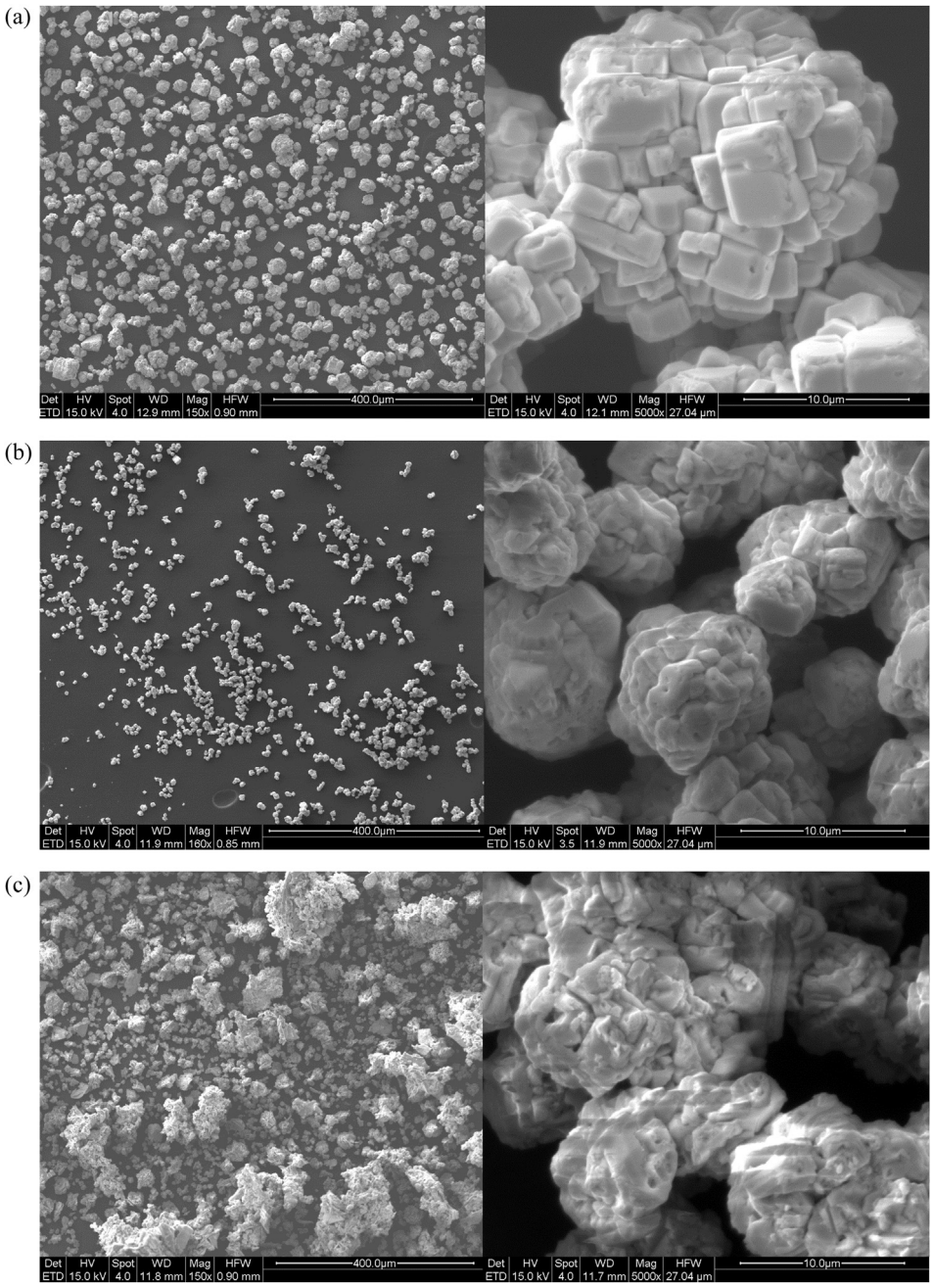

Fig. 2. SEM images of $Bi_{1-x}La_xFeO_3$ a) $x = 0.15$), b) $x = 0.30$ and c) $x = 0.45$ particles for selected samples.

show an homogenous size distribution with a semi-cubic morphology in spherical aggregates characterized by a mean diameter of 20 μm (Fig. 2a). After the lanthanum doping with x = 0.15 (Fig. 2b), the diameter of particles is reduced to an average diameter of 5 μm in a homogeneous size distribution. When the La doping level increases up to x = 0.45 (Fig. 2c) the particles show irregular shape agglomerates of 10 μm and/or hundred micrometers. Hence, the particle morphologies and size indicate that the doped lanthanum ion has an effect on the crystallization habit of $BiFeO_3$ particles in a microwave assisted hydrothermal method.

3.3. Thermal characterization

To characterize the thermal behaviour of the perovskite-structured particles Fig. 3a shows the TGA curves for all the prepared samples. The weight losses appear as a sequence of losses that occurred at nearly identical temperatures in all samples, namely at about 120 °C, 250–400 °C, 460–500 °C, 600 °C, 670 °C, 750 °C and a larger weight loss starting at 850 °C, which is likely attributed to decomposition and evaporation of Bi_2O_3. As seen from the first derivative of the weight loss (DTG) in the figure, weight losses at 260–320 °C and particularly at 850 °C were relatively larger for the two higher doping levels than for the two less doped materials. In particular, the highest doping level exhibited higher weight losses in most of the steps.

The differential temperature (DTA) has been shown in Fig. 3b–c. In all the curves endothermic peaks can be found at about 120 °C, 300–320 °C, 420 °C, 800–815 °C and 850 °C, whereas the DTA-peak associated with the weight losses between 400 and 500 °C seems to be exothermic. Up to 200 °C only the $Bi_{0.55}La_{0.45}FeO_3$ sample

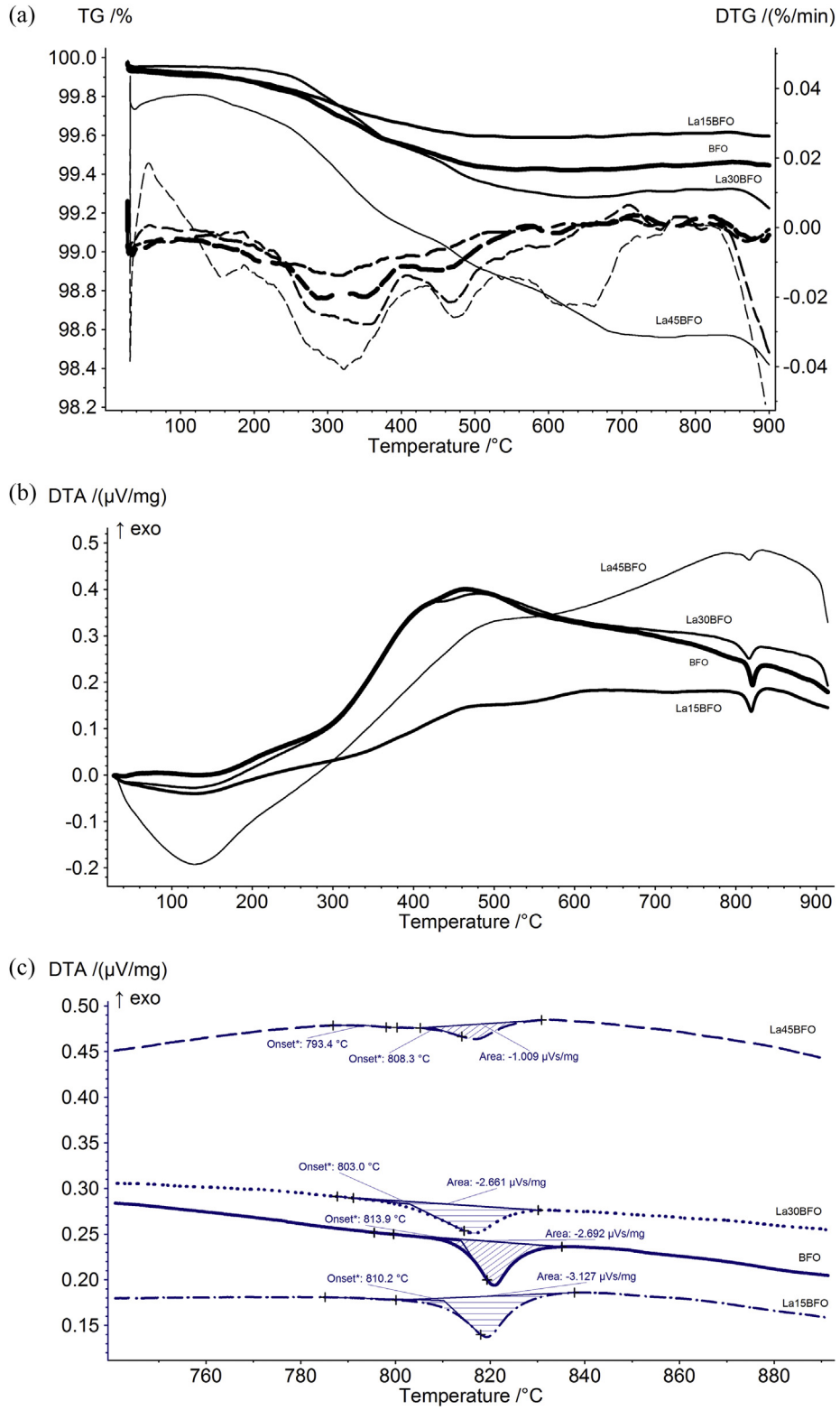

Fig. 3. a) TG/DTG trace observed for $Bi_{1-x}La_xFeO_3$ $0 \leq x \leq 0.45$ heated at a constant rate 10 C/min up to 900 °C in nitrogen atmosphere; b) simultaneous DTA pattern and c) DTA enlargement in the range between 700 °C and 900 °C for all the prepared samples.

presents an endothermic peak at around 187.7 °C, but it is not related to any significant loss of weight. In the pure sample $BiFeO_3$, an endothermic peak can be seen at about 330 °C attributed to the Neél temperature of BFO [9]. Based on the literature, the small endothermic peak at around 815 °C could be assigned to a ferroelectric-to-paraelectric phase transition [23], which has been enlarged in Fig. 3c where a significant shift in the transition temperature from 814 °C to about 793 °C as function of the La-doping is observed. Table 1 reports the numbers of extrapolated onset temperatures T_C (Curie temperature), and peak area for all the

Table 1
Numbers of extrapolated onset and peak area for all the $Bi_{1-x}La_xFeO_3$ $0 \leq x \leq 0.45$ investigated powders (RT = room temperature).

	Extrapolated onset, T_C °C	Peak area, μVs/mg (heat–cool segments)	Extrapolated onset, °C	Weight loss, RT-900 °C
BFO	813.9	2.69–2.94		0.51%
$La_{0.15}Bi_{0.85}FeO_3$	810.2	3.13–3.49		0.33%
$La_{0.30}Bi_{0.70}FeO_3$	803.0	2.66–0.82		0.73%
$La_{0.45}Bi_{0.55}FeO_3$	808.3	1.01–na	793.4	1.39%

investigated powders. The T_C is 813.9 °C for undoped BFO and it decreases with La doping increase. The two formulations with x = 0 and 0.15 retained both the peak-shape and the peak area during the cooling segment, while at higher doping levels a secondary peak started to develop at lower temperatures. This phenomenon can better be seen on the trace of the $La_{0.45}Bi_{0.55}FeO_3$ and it has been highlighted in Table 1 by two values for the extrapolated onset during heating. In addition to the phase transition, samples showed minor weight losses (Table 1). Again, pure BFO and BLFO with x = 0.15 behave more or less identical, whereas the two higher doping levels lead to markedly higher degradation summarizing the DTA–TGA results suggest that the La 15% doping of BFO was successful, while higher doping levels lead to gradually lower thermal stability and phase purity.

3.4. Crystal structure characterization

Starting from the characterizations yet reported it is evident that all the samples have shown a single crystalline phase without impurity phases (XRD analysis, Fig. 1a), but at doping levels greater than x = 0.15 the samples, keeping the same crystalline pattern, seems to undergo structural distortions highlighted by morphological characterizations (Fig. 2) and by thermal analysis (Fig. 3). For these reasons the work has been concluded with the Raman and magnetic characterization of $La_{0.15}Bi_{0.85}FeO_3$.

The details of iron and bismuth chemical environments have been studied by Raman spectra illustrated in Fig. 4. The presence of Raman-active modes can be used to evaluate the structural order degree at short-range. The modes below 200 cm^{-1} in Fig. 4a were addressed to different sites occupied by bismuth within the perovskite units, in accordance to [9]. The bands located at approximately 65, 127 and 162 cm^{-1} are related to Bi atoms of peroskite layer and corresponds E_1(1LO), A_1(1TO), A_1(2TO) respectively [9]. In addition, the modes recorded above the 200 cm^{-1} are caused by internal vibration of FeO_6 octahedra. Raman frequencies are not strongly affected by lanthanum substitution. In fact, it is worthwhile to note that the Raman spectrum of the $La_{0.15}Bi_{0.85}FeO_3$ sample Fig. 4b showed the same BFO bands, even though with decreasing intensities and a slight shift towards lower frequencies. This displacement is likely due to the substitution of the bismuth atom by lanthanum into the BFO lattice [9].

3.5. Magnetic characterization

Fig. 5 presents the magnetization as a function of field at room temperature for BFO and $La_{0.15}Bi_{0.85}FeO_3$ measured as full loops (1.5T -> −1.5T -> 1.5T). The results show the expected antiferromagnetic behaviour with a weak ferromagnetic component due to crystalline or structural imperfections of the investigated samples: the magnetization of the doped sample is slightly lower than the

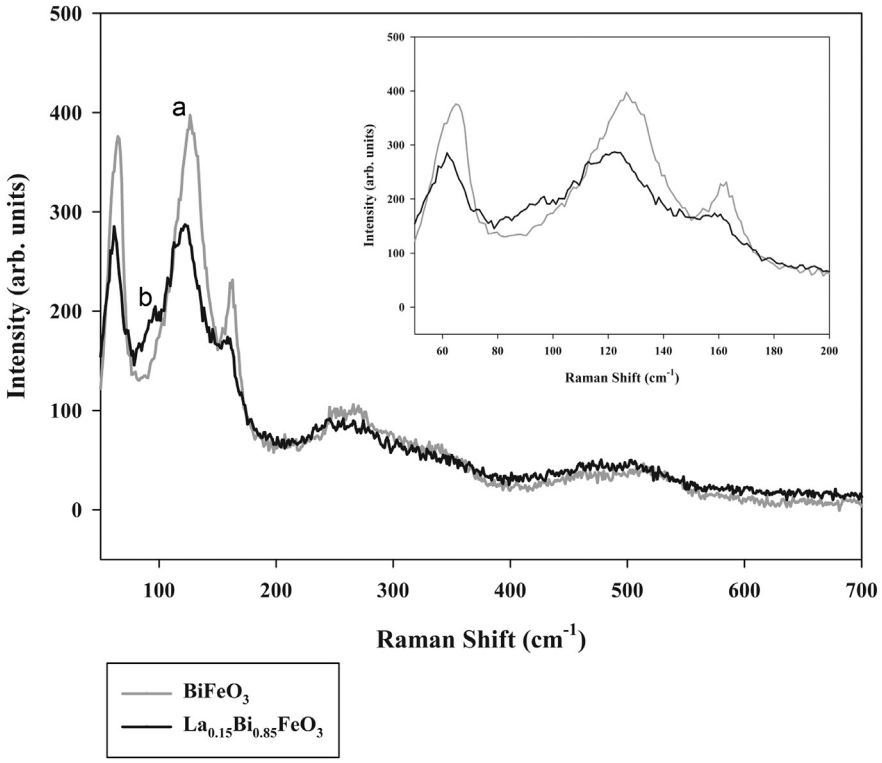

Fig. 4. Raman spectra for $Bi_{1-x}La_xFeO_3$ powder with a) x = 0 and the b) x = 0.15, synthesized using 8 M KOH at 200 °C for 30 min.

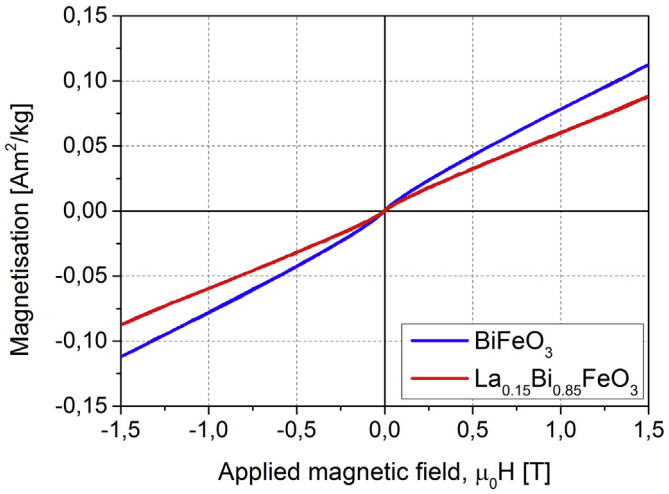

Fig. 5. Variation of magnetization as a function of field measured at room temperature for BFO and $La_{0.15}Bi_{0.85}FeO_3$.

undoped one. Furthermore, it is clear that there is no significant hysteresis in either sample. In fact, the hysteresis in the studied materials is a mere 0.01 T, which is close to the instrumental resolution of the VSM used.

4. Discussion & conclusions

Lanthanum-doped bismuth ferrite ($Bi_{1-x}La_xFeO_3$, x = 0, 0.15, 0.30, and 0.45) crystallites were successfully synthesized by an ultrafast microwave assisted hydrothermal method. The optimized microwave hydrothermal conditions allowed to promote the formation of crystalline BLFO powders at a very low processing temperature of 200 °C, which greatly reduced the synthesized temperature by about 500 °C and reaction time for the BLFO phase in comparison with the conventional sol–gel process. Moreover when a conventional hydrothermal synthesis is applied the reaction temperatures are similar, but the reaction time is significantly longer than the microwave assisted hydrothermal approach. Pure $Bi_{1-x}La_xFeO_3$ crystallites could be obtained when $x \leq 0.45$ as suggested by XRD patters, but $x = 0.15$ represents the doping threshold beyond which a perovskite degradation has taken place in terms of the thermal properties (TG/DTA) and morphology (ESEM images). Indeed the ferroelectric transition temperature decreased from 813.9 to 803 °C with increasing La doping and size distribution. The morphologies changed from homogenous semi-cubic in spheroidal aggregates with a size around 20 μm for undoped particles and with 2 μm for $x = 0.15$ doped particles to an irregular shape with several 10 and/or hundred μms for higher doping levels. Moreover the Raman spectroscopy confirmed that the $La_{0.15}Bi_{0.85}FeO_3$ is characterized by bismuth and iron chemical environments similar to the undoped bismuth ferrite. Even though some differences between BFO and $x = 0.15$ doped samples were observed, any significant variation at room temperature in the magnetic moment was seen.

As conclusive remark we can state that this paper shows that the microwave assisted hydrothermal route, without the presence of catalysts and expensive equipment, has been able to ensure high purity in the products and greatly reduce the production cost. Therefore this approach offers a novel, fast and simple synthetic route for high-quality mixed oxide ceramic powders.

Acknowledgements

This work was financially supported by CNR PAR2011-12.

References

[1] G. Catalan, J.F. Scott, Adv. Mater. 21 (2009) 2463–2485.
[2] W. Eerestein, N.D. Mathur, J.F. Scott, Nature 442 (2006) 759–765.
[3] N.A. Spaldin, M. Fiebig, Science 309 (2005) 391–392.
[4] J. Wang, J.B. Neaton, H. Zheng, V. Nagarajan, S.B. Ogale, B. Liu, D. Viehland, V. Vaithyanathan, D.G. Schlom, U.V. Waghmare, N.A. Spaldin, K.M. Rabe, M. Wuttig, R. Ramesh, Science 299 (2003) 1719–1722.
[5] K.Y. Yun, M. Noda, M. Okuyama, Appl. Phys. Lett. 83 (2003) 3981–3984.
[6] S. Li, Y.H. Lin, B.P. Zhang, Y. Wang, C.W. Nan, J. Phys. Chem. C 114 (7) (2010) 2903–2908.
[7] C. Ponzoni, R. Rosa, M. Cannio, V. Buscaglia, E. Finocchio, P. Nanni, C. Leonelli, J. Eur. Cer. Soc. 33 (7) (2013) 1325–1333.
[8] J. Deng, S. Banerjee, S.K. Mohapatra, Y.R. Smith, M. Misra, J. Fundam. Renew. Energy Appl. 1 (2011) 1–10.
[9] F.G. Garcia, C.S. Riccardi, A.Z. Simões, J. Alloys Compd. 501 (2010) 25–29.
[10] S.T. Zhang, Y. Zhang, M.H. Lu, C.L. Du, Y.F. Chen, Z.-G. Liu, Y.Y. Zhu, N.B. Ming, X.Q. Pan, Appl. Phys. Lett. 88 (2006) 162901–162904.
[11] G.L. Yuan, O.S. Wing, J. Appl. Phys. 100 (2006) 024109–024120.
[12] S.K. Singh, H. Ishiwara, Jpn. J. Appl. Phys. 45 (2006) 3194–3197.
[13] J.K. Kim, S.S. Kim, W.J. Kim, Mater. Lett. 59 (2005) 4006–4009.
[14] S. Ghosh, S. Dasgupta, A. Sen, H.S. Maiti, J. Am. Cer. Soc. 88 (2005) 1349–1352.
[15] A. Chaudhuri, S. Mitra, M. Mandal, K. Mandal, J. All. Comp. 491 (2010) 703–706.
[16] S.H. Han, K.S. Kim, H.G. Kim, H.G. Lee, H.W. Kang, J.S. Kim, C.I. Cheon, Ceram. Intern. 36 (2010) 1365–1375.
[17] Z.W. Chen, G.H. Zhan, X.H. He, H. Yang, H. Wu, Cryst. Res. Technol. 46 (2011) 309–314.
[18] A. Chaudhuri, K. Mandal, Mat. Res. Bull. 47 (2012) 1057–1061.
[19] J. Prado-Gonjal, M.E. Villafuerte-Castrejón, L. Fuentes, E. Moran, Mat. Res. Bull. 44 (2010) 1734–1737.
[20] C. Ponzoni, R. Rosa, M. Cannio, V. Buscaglia, E. Finocchio, P. Nanni, C. Leonelli, J. Alloys Compd. 558 (2013) 150–159.
[21] A. Rizzuti, C. Leonelli, Process. Appl. Ceram. 3 (1–2) (2009) 29–32.
[22] Z. Chen, Y. Li, Y. Wu, J. Hu, J. Mater. Sci. 23 (2012) 1402–1408.
[23] A. Perejón, P.E. Sánchez-Jiménez, L.A. Pérez-Maqueda, J.M. Criado, J. Romero de Paz, R. Sáez-Puche, N. Masó, A.R. West, J. Mater. Chem. C 2 (2014) 8398–8411.